Stem Cell Reports
Article

ISSCR

OPEN ACCESS

Early Depletion of Primordial Germ Cells in Zebrafish Promotes Testis Formation

Keh-Weei Tzung,[1,7,*] Rie Goto,[2,7,8] Jolly M. Saju,[1] Rajini Sreenivasan,[1,9,10] Taiju Saito,[2,11] Katsutoshi Arai,[3] Etsuro Yamaha,[2] Mohammad Sorowar Hossain,[1,12] Meredith E.K. Calvert,[4] and László Orbán[1,5,6,*]

[1]Reproductive Genomics Group, Strategic Research Program, Temasek Life Sciences Laboratory, Singapore 117604, Singapore
[2]Nanae Fresh Water Laboratory, Field Science Center for Northern Biosphere, Hokkaido University, Nanae, Kameda, Hokkaido 041-1105, Japan
[3]Faculty of Fisheries Sciences, Hokkaido University, Hakodate, Hokkaido 041-8611, Japan
[4]Bioimaging and Biocomputing Facility, Temasek Life Sciences Laboratory, Singapore 117604, Singapore
[5]Department of Animal Sciences and Animal Husbandry, Georgikon Faculty, University of Pannonia, 8360 Keszthely, Hungary
[6]Centre for Comparative Genomics, Murdoch University, Murdoch, WA 6150, Australia
[7]Co-first author
[8]Present address: Nishiura Station, South Ehime Fisheries Research Center, Ehime University, Uchidomari, Ainan, Ehime 798-4206, Japan
[9]Present address: Molecular Genetics and Development Division, MIMR-PHI Institute of Medical Research, Clayton, VIC 3168, Australia
[10]Present address: Department of Anatomy and Neuroscience, University of Melbourne, Parkville, VIC 3010, Australia
[11]Present address: Research Institute of Fish Culture and Hydrobiology, Faculty of Fisheries and Protection of Waters, University of South Bohemia in České Budějovice, 389 25 Vodňany, Czech Republic
[12]Present address: Biotech Division, Incepta Pharmaceuticals, Ltd., Dhaka 1208, Bangladesh
*Correspondence: kehweei.tzung@gmail.com (K.-W.T.), laszlo@tll.org.sg (L.O.)
http://dx.doi.org/10.1016/j.stemcr.2014.10.011

SUMMARY

As complete absence of germ cells leads to sterile males in zebrafish, we explored the relationship between primordial germ cell (PGC) number and sexual development. Our results revealed dimorphic proliferation of PGCs in the early zebrafish larvae, marking the beginning of sexual differentiation. We applied morpholino-based gene knockdown and cell transplantation strategies to demonstrate that a threshold number of PGCs is required for the stability of ovarian fate. Using histology and transcriptomic analyses, we determined that zebrafish gonads are in a meiotic ovarian stage at 14 days postfertilization and identified signaling pathways supporting meiotic oocyte differentiation and eventual female fate. The development of PGC-depleted gonads appears to be restrained and delayed, suggesting that PGC number may directly regulate the variability and length of gonadal transformation and testicular differentiation in zebrafish. We propose that gonadal transformation may function as a developmental buffering mechanism to ensure the reproductive outcome.

INTRODUCTION

Primordial germ cells (PGCs) are the stem cells of the gametes, providing genome transmission to future generations (Lesch and Page, 2012). During development, PGCs undergo specification, migration, and proliferation. Reciprocal interactions between germ cells and somatic cells are important for gonadal differentiation (Kocer et al., 2009). However, little is known about the regulatory role of germ cells during sexual development.

In mammals, agametic male gonads develop into a normal testis cord, while loss of germ cells in ovaries at birth disrupts ovarian structures and folliculogenesis (Merchant-Larios and Centeno, 1981). In teleosts, the requirement of germ cells for gonadal development appears to be variable. Their absence leads to exclusive male development in medaka and zebrafish (Kurokawa et al., 2007; Siegfried and Nüsslein-Volhard, 2008; Slanchev et al., 2005), but not in goldfish or loach (Fujimoto et al., 2010; Goto et al., 2012).

Mammalian sex determination is regulated by antagonistic pathways, which direct the bipotential embryonic gonad toward ovarian or testicular fate (Warr and Greenfield, 2012). Moreover, evidence indicates that somatic sex needs to be reinforced throughout adulthood. In mice, loss of FOXL2 in mature ovary or DMRT1 in mature testis causes transdifferentiation of somatic cells (Matson et al., 2011; Uhlenhaut et al., 2009). In zebrafish, oocytes appear essential for the development of females in juveniles and for maintenance of the sexual phenotype in adults (Dranow et al., 2013).

The number of PGCs likely plays an important role in teleost sexual differentiation. For medaka and stickleback, females possess more germ cells than males due to their sexually dimorphic proliferation (Lewis et al., 2008; Saito et al., 2007). Transplantation of a single PGC into a germline-deficient zebrafish embryo generates males exclusively (Saito et al., 2008). *ziwi* mutants with reduced PGC numbers can develop as males or females; however, a greater reduction due to a hypomorphic allele in *trans* to a null allele gives rise to males (Houwing et al., 2007). These data argue that the absolute number of germ cells is important in determining the sexual phenotype of zebrafish.

Zebrafish are undifferentiated gonochorists since all individuals first initiate oogenesis via forming an immature ovary (Takahashi, 1974). In developing males, but not in

females, a gonad transformation arises from apoptosis-driven degeneration of oocytes (Uchida et al., 2002; Wang and Orban, 2007) about 23–35 days postfertilization (dpf) leading to subsequent testis development (Orban et al., 2009; Uchida et al., 2002). Molecular control of sex determination and gonad differentiation in zebrafish appears to be complex (Liew and Orban, 2014; Orban et al., 2009) and variable across domesticated strains versus wild populations (Liew et al., 2012; Wilson et al., 2014).

In this study, we analyze the relationship between the number of PGCs and sexual differentiation in zebrafish. By tracking changes in the PGC number during development, we demonstrate that a dimorphic proliferation of PGCs occurs in the early larvae, underlining the beginning of sexual differentiation. By creating zebrafish containing various numbers of PGCs, we show that a threshold number of PGCs is required for stabilizing the ovarian fate and that PGC number may directly regulate the progression of gonadal transformation.

RESULTS

Dimorphic Proliferation of PGCs Occurred during Early Larval Stages in Zebrafish

To understand how the PGC count might be involved in sexual differentiation, we examined their numbers at different development stages using the *Tg(vasa:vasa-EGFP)* (i.e., *zf45Tg*) transgenic zebrafish line (Figure 1A). For clarity, the term "PGC" was used before 2 weeks of zebrafish development. First, we estimated the number of PGCs present in the gonadal region between 1 dpf and 8 dpf with the squash method. The number of PGCs ranged from 25 to 44 at 1 dpf, without obvious fluctuations in the PGC number during the first week of development (Figure 1B).

Next we used optical sectioning to precisely count PGC numbers at 7 and 14 dpf in WT larvae from two different families (FI and FII). The PGC count at 7 dpf appeared to follow a unimodal distribution (Figure 1C). At 14 dpf, the number of PGCs showed a bimodal distribution between two distinct populations (means = 40.3 ± 7.7 and 87.7 ± 12.1; Figure 1D), and the difference between the means was significant (Student's t test, $p < 0.05$). Morphologically, green fluorescent protein (GFP)-expressing gonadal regions exhibited a smaller and less dense morphology at 7 dpf (Figure 1E) and became larger as the number of GFP-expressing cells increased at 14 dpf. In 14 dpf individuals with a higher number of PGCs, gonadal regions were broader and denser due to the increased number of cells populating that region (Figures 1F and 1G). To determine whether this bimodal distribution in PGC number was due to a family-specific effect, we examined the distribution of PGC number by family. Intriguingly, 83.3% of individuals in FI, the family with a slightly female-biased offspring sex ratio (60%), exhibited gonadal regions with a higher number of PGCs, while nearly 60% of individuals in the male-biased FII (84%) contained a lower number of PGCs at 14 dpf (Figures 1H and 1I). Our data suggest that a dimorphic proliferation of PGCs occurs between 7 and 14 dpf and that progeny sex ratios within families may correlate with the divergent distribution of PGC numbers.

Depletion of PGCs in the Embryos Resulted in Masculinization of Zebrafish Gonads

To further investigate whether there was a relationship between early PGC count and sexual development, we compared unmanipulated *Tg(vasa:vasa-EGFP)* individuals with low PGC and high PGC counts and found no difference in their trunk-based expression at 22 dpf (Figure S1A available online) or adult sex ratio (Figure S1B). Next, we generated zebrafish morphants with depleted PGCs using two different methods. In the first approach, we microinjected a diluted morpholino oligonucleotide (MO) directed against the *dead end* gene (*dnd*) into *Tg(vasa:vasa-EGFP)* zebrafish embryos. Injected embryos were categorized based on the PGC number observed at 24–32 hours postfertilization (hpf) and then grown to adulthood together with uninjected embryos (control), and sexual phenotype was assessed.

Next, we used optical sectioning to count PGC numbers in *dnd* morphants at 7 and 14 dpf. In the majority of larvae from zero PGC and severely depleted PGC groups (PGC count <6 at 24–32 hpf), gonadal structures were absent (Figures 2A and 2B), and these individuals were excluded from further microscopic analysis. In the remaining PGC-depleted group (PGC count 6–9 at 24–32 hpf), the majority of the larvae at 7 and 14 dpf had loose aggregates of PGCs, but were lacking clear gonadal structures. Of the undepleted gonads (>20 PGCs at 24–32 hpf), more than 60% showed clear gonadal structures at 7 dpf.

Among larvae with visible PGCs, the average PGC number was 7.8 ± 4.8 in the PGC-depleted gonads (6–9) and 29.1 ± 9.4 in undepleted gonads (>20) at 7 dpf. At 14 dpf, the morphology of PGC-depleted gonads was similar to those in 7 dpf; however, all of the larvae with undepleted gonads (>20) exhibited distinct gonadal structures (Figure 2B). The average PGC number was 25.6 ± 16.8 in PGC-depleted gonads; in contrast, the PGC count in undepleted gonads displayed a bimodal distribution comparable to that observed in uninjected larvae (means = 47.4 ± 9.8 and 99.3 ± 20.9; Figure 2C, right). This suggested that morpholino-induced PGC depletion below a threshold effectively prevented subsequent PGC proliferation in most individuals and that the effect was maintained during later stages.

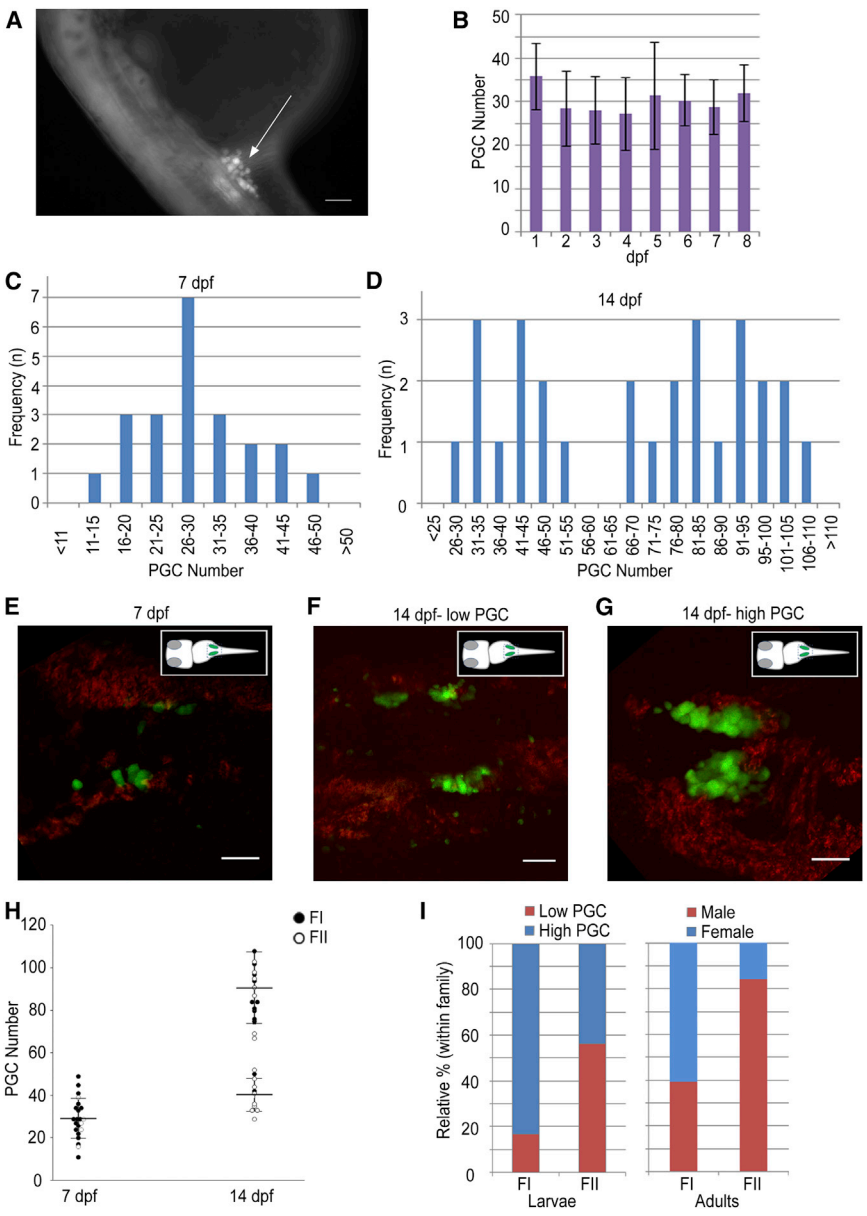

Figure 1. Dimorphic Proliferation of PGCs Happens during the Second Week in the Larval Gonads of the Zebrafish

(A) A 24 hpf embryo of the *Tg(vasa:vasa-EGFP)* transgenic line. The GFP (+) germ cells cluster around anterior part of the yolk extension (arrow). The scale bar represents 100 μm.

(B) The PGC number in the first 8 days of development counted using the squash method. Image and PGC counts obtained using a compound epifluorescence microscope (n = 10, 10, 12, 6, 5, 3, 4, and 3 at 1–8 dpf, respectively). The mean ± SD is shown.

(C and D) Frequency distribution of PGC number at (C) 7 dpf (n = 22) and (D) 14 dpf (n = 28), showing unimodal and bimodal distributions, respectively.

(E–G) Trunk regions of the *Tg(vasa:vasa-EGFP)* line, showing different PGC distributions at 7 and 14 dpf. Images are average intensity projections of confocal z stacks showing GFP (+) cells (green) and background autofluorescence (red). Scale bars represent 50 μm.

(H) Density dot plot showing changes in the PGC number during development between different mating pairs (FI, closed circles; FII, open circles) at 7 and 14 dpf. Large horizontal bars indicate mean; smaller flanking bars indicate SD.

(I) Relative percentages of individuals in low (<60, red) and high (>65, blue) PGC number groups within families (FI, n = 12; FII, n = 16) at 14 dpf (left) and the respective progeny sex ratios (male, red; female, blue; FI, n = 194; FII, n = 138).

After 3 months postfertilization (mpf), the sex ratios of the *dnd* morphants were evaluated. For both pairwise cross (MO1) and mass cross (MO2), the "zero PGC" group produced exclusively males as expected based on published data (Slanchev et al., 2005). Their gonads were empty testicular shells completely devoid of germ cells confirming earlier data (Siegfried and Nüsslein-Volhard, 2008). A strong male-biased sex ratio (mean = 90% in four batches for MO1 and 76% in six batches for MO2) was identified in PGC-depleted groups (1–10 PGCs for MO1, 1–7 for MO2) (Figure 2D). These results suggested that—similar to the minimum PGC number required for proliferation—a certain number of PGCs seems to be necessary for unaffected ovarian development in most individuals. Individuals with severely depleted PGCs (1–5), excluded from the morphological analysis, all developed into fertile males with a gonadal histology similar to WT males and were included in the subsequent transcriptomic analysis.

To further explore the correlation between PGC number and the phenotypic sex of fish using a different approach, we applied both single PGC transplantation (SPT; Figure 3A) and blastoderm transplantation (BdT; Figures 3B–3G and 3I–3K) for generating germline chimeras. Both procedures utilize sterilized, PGC-less host embryos. GFP-labeled PGCs were used for SPT and GFP-tagged blastodermal cells (containing DsRed-expressing PGCs) were applied for BdT. In general, SPT results in a germline chimera possessing a single PGC, whereas BdT yields individuals with variable

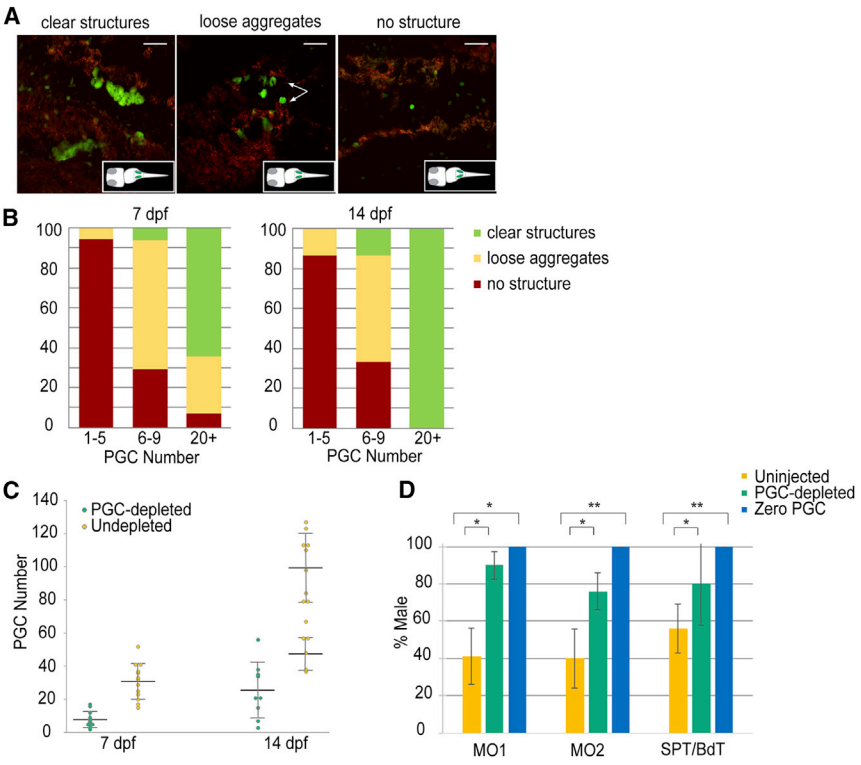

Figure 2. Masculinization Ensues in PGC-Depleted Zebrafish

(A) Representative images of gonads show morphological variants following PGC depletion. Images are average intensity projections of confocal z stacks showing GFP (+) cells (green) and background autofluorescence (red). Scale bars represent 50 μm.

(B) The relative percentage of morphological variants observed during development based on resultant PGC number at 7 and 14 dpf following depletion.

(C) Density dot plot showing the stage-specific PGC number in PGC-depleted (6–9 PGCs, green; 7 dpf, n = 17 and 14 dpf, n = 15) and undepleted (>20 PGCs, yellow; 7 dpf, n = 14 and 14 dpf, n = 16) larvae. The resultant PGC number at 14 dpf in PGC-depleted larvae shows a unimodal distribution, while remaining bimodal in the undepleted ones. Large horizontal bars indicate mean; smaller flanking bars indicate the SD.

(D) Relative percentage of male progeny resulting from two different methods of PGC-depletion: morpholino injection-MO1 (pairwise cross), MO2 (mass cross), and cell transplantation-SPT, BdT. The bar color indicates resultant PGC number zero (blue: n = 27, 29, 159 for MO1, MO2, and SPT/BdT), PGC-depleted (1–10 for MO1, 1–7 for MO2 and 1–9 for SPT/BdT, green; n = 111, 97, and 50 for MO1, MO2, and SPT/BdT) and uninjected controls (yellow: n = 237, 364, and 136 for MO1, MO2, and SPT/BdT). Bars indicate mean % ± SD of the mean percentages in four, six, four, and eight replicated experiments for MO1, MO2, SPT, and BdT, respectively. t test: *$p < 0.01$; **$p < 0.001$ calculated when PGC-depleted versus uninjected or zero PGC versus uninjected.

See also Figures S1 and S2.

number of donor-derived PGCs in the early gonad. PGC counts for the latter are typically much lower than those observed in uninjected controls.

In SPT chimeras, a single PGC was present at the gonadal regions of 20.7% of the host embryos at the prim-5 stage (Figure 3A) and all developed as males. For BdT chimeras, transplanted donor-derived cells were mixed with PGC-depleted host cells uniformly at the prim-5 stage, and most donor PGCs were recognized as red fluorescent cells around the gonadal ridge (3–29 cells; Figures 3B–3D; see also Movies S1 and S2). A total of 109 BdT germline chimeras survived to adulthood (see Table S1 for details), at which point identification of the two sexes was performed based on phenotype and/or dissection of their gonads; both female and male chimeras showed mosaic GFP fluorescence and regional red fluorescent protein (RFP) fluorescence (Figures 3F, 3G, 3J, and 3K). Nearly 80% of BdT recipients developed as males in the PGC-depleted group (1–9) (Figure 2D). Representative gonads from female and male BdT chimeras were subjected to histological analysis and showed completely developed gonads indistinguishable from those of controls (Figures 3H and 3L). Although examined gonads of SPT chimeras showed an intact testis only on one side, these fish were sexually active and fertile. None of the "zero PGC" morphants possessed fully developed, fertile gonads.

It was noted that ~10%–20% of PGC-depleted individuals (initial PGC count 1–9) still developed as females (Figure 2D). Taken together, our data show when the PGC number is artificially lowered below a threshold, a substantial portion of genetic females will be forced through masculinization, increasing the proportion of males among the offspring.

Zebrafish Gonads Were in a Meiotic Stage at 14 dpf

To understand how a reduced PGC number might influence sexual differentiation in zebrafish, we used a microarray-based approach to investigate differences between the transcriptomes of PGC-depleted (1–9 PGCs) versus WT larvae. We collected samples from developing trunk regions for histology and gene expression profiling.

At 14 dpf, WT samples clustered into two groups based on principal component analysis (PCA; Figure 4A), and seven genes were differentially expressed (DE; >2-fold, $p < 0.05$;

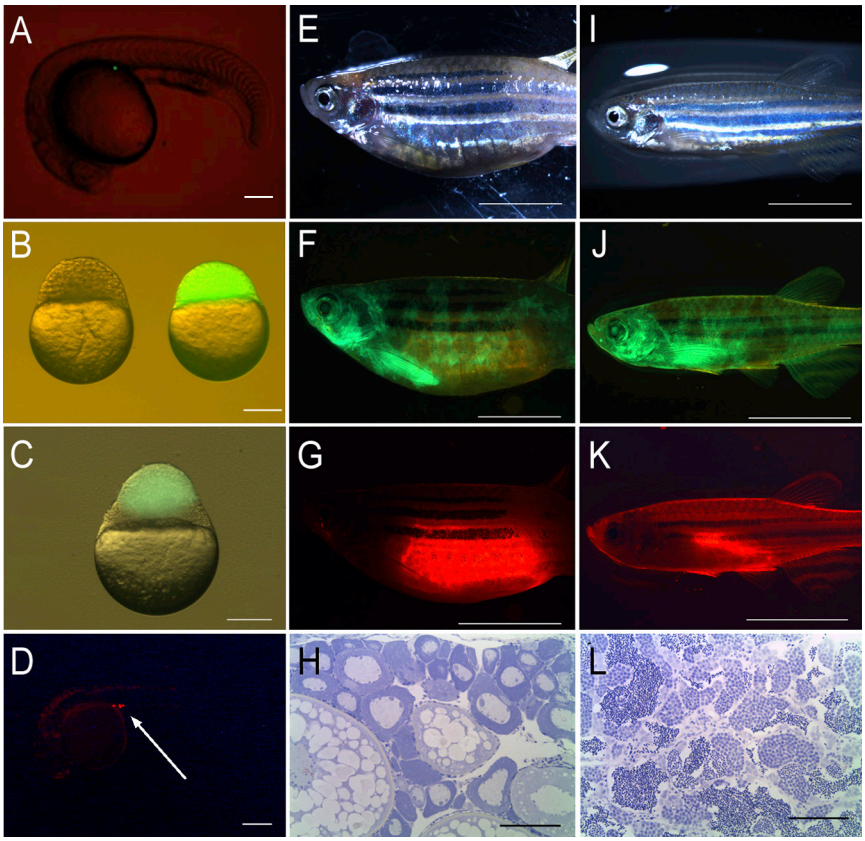

Figure 3. Germline Chimeras Produced by Cell Transplantation, SPT and BdT, in Zebrafish

(A) A single PGC with GFP fluorescence located at the gonadal ridge in a SPT chimera at the 25 somite stage.

(B) The recipient of golden zebrafish (left) and the donor of *Tg*(*vasa:DsRed2-vasa*); *Tg*(*bactin:EGFP*) double transgenic embryos (right) used for the generation of BdT chimeras.

(C) A donor blastoderm with GFP fluorescence attached to the host blastoderm a few hours after transplantation.

(D) Donor-derived PGCs with RFP fluorescence were at the gonadal ridge at the prim-5 stage in a BdT chimera (arrow).

(E–L) Representative female (E–G) and male (I–K) BdT chimeras were imaged under bright field (E and I), GFP fluorescence (F and J), and RFP fluorescence (G and K). Histological analysis of selected gonads (n = 5) from germline chimeras confirmed the presence of an ovary (H) or a testis (L).

Scale bars represent 20 μm (A–D), 500 μm (E–G and I–K), and 100 μm (H and L). See also Table S1 for the survival rates following these manipulations and Movies S1 and S2 for BdT.

see Table S2 for gene names and Table S3 for a selected set of DE genes). Among them were genes involved in cell-cycle regulation (*fbxl18*, *cdkn2aipnl*, and *cbx3*), consistent with our observation that bimodal proliferation of PGCs occurs between 7 and 14 dpf.

The comparison of transcriptomes between WT and PGC-depleted samples indicated that the latter (cluster 1) did not group closely with WT samples (clusters 2 and 3; Figure 4A), suggesting the differences in transcriptome between PGC-depleted individuals and the future WT males. Further gene expression analysis showed 134 DE genes when comparing combined WT clusters (2 and 3) to cluster 1 (Table S3). Among them, 102 genes were upregulated, and 32 genes were downregulated in WT compared with PGC depleted (Figure 4B; see Table S4 for a selected set of DE genes). Gene ontology (GO) analysis identified gene clusters of meiosis, cell-cycle regulators, immune response, and germ/stem cell genes among those in this DE group. In particular, meiotic genes (*dazl*, *hormad1*, *smc1b*, and *sycp2*) were downregulated, whereas most genes with immune related function (*irf8*, *cd209*, and *ccl1*) were upregulated in the PGC-depleted group compared with WT. In addition, potential ovarian (*org*) and testicular (*rnf17*) markers were expressed at higher levels in the WT group. Our data suggested that (1) the trunk-based transcriptome of PGC-depleted individuals shows clear differences from those of their WT siblings, (2) WT zebrafish gonads are in a meiotic stage at 14 dpf, and (3) entry into meiosis might be an important early step in ovarian differentiation.

Multiple Sexual States Were Present during Gonadal Transformation at 22 dpf

At 22 dpf, gene expression data indicated that WT samples could be divided into two clusters based on PCA, with 945 DE genes (>2-fold, $p < 0.05$). When WT and PGC-depleted samples were compared through a PCA plot, five distinct clusters were formed, suggesting that different transitional states of gonads might be present. All WT individuals fell into clusters 1–4, whereas PGC-depleted individuals remained in cluster 5. For analytical purposes, cluster 1 was assigned as "immature females," clusters 2–4 as WT transforming (female-to-male), and cluster 5 as PGC-depleted transforming individuals (Figure 4C). To find genes with a potential function in early gonad differentiation and/or testis formation, we compared "immature females" (cluster 1) with a subset of WT and PGC-depleted transforming males (clusters 4 and 5). A total of 1,329 DE genes was identified (>2-fold, $p < 0.05$; Table S3). Among them, 1,136 genes were upregulated in "immature females," and 193 genes were overexpressed in future males (Figure 4D).

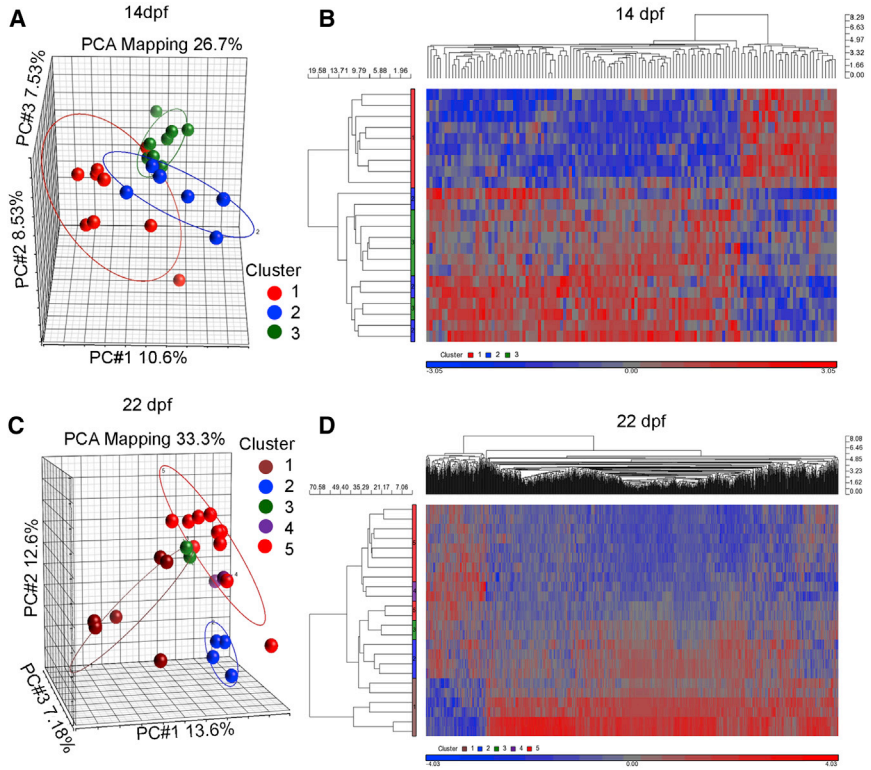

Figure 4. Transcriptome Characteristics of Zebrafish Gonads with Partially Depleted and WT PGCs Demonstrate the Divergence of WT Individuals and Clustering between WT and PGC-Depleted Transforming Males at Different Developmental Stages

(A) At 14 dpf, the PCA plot showed that PGC-depleted samples (1–9; cluster 1, red) did not group closely with WT samples (clusters 2 and 3, blue and green, respectively).

(B) The heatmap of hierarchical clustering of 132 DE genes at 14 dpf between PGC-depleted and WT (>2-fold, $p < 0.05$) showed cluster 1 separated from clusters 2 and 3.

(C) At 22 dpf, the PCA plot showed several distinct clusters, suggesting the high variability in the transformation process from females to males. Cluster 1 was assigned as immature female. Clusters 2, 3, and 4 were assigned as transforming gonads from female to male, and cluster 5 was assigned as PGC-depleted transforming male.

(D) The heatmap produced by hierarchical clustering of 1,329 genes that showed differential expression at 22 dpf when cluster 1 was compared with clusters 4 and 5 (>2-fold, $p < 0.05$). As shown, cluster 4 was grouped with cluster 5 (PGC-depleted male); cluster 3 displayed a transitional pattern and was closer to cluster 5.

See also Table S2 for a list of gene symbols and names, Table S3 for a list of DE genes, and Table S4 for functional classification of DE genes.

Unlike at 14 dpf, where PGC-depleted samples showed separation from WT individuals, two of the unmanipulated samples (very likely the most advanced transforming males from cluster 4) coclustered with PGC-depleted individuals at 22 dpf (Figure 4C). This indicated that the expressed gene set of WT males and PGC-depleted males became more similar to each other by 22 dpf. To gain insight into possible biological functions of these genes, they were sorted into signaling pathways based on the KEGG or PANTHER classification system (Kanehisa et al., 2012; Mi et al., 2013).

The Importance of Transforming Growth Factor β Signaling for Meiotic Progression and Folliculogenesis in Developing Zebrafish Gonads

In "immature females" (cluster 1), cohorts of genes associated with cell cycle, cell death, and metabolism were upregulated, indicating active remodeling of tissue architecture and morphogenesis. Detailed analysis of this cluster identified genes related to germ/stem cell markers (*pou5f1*, *lin28a*, *nanog*, *nfr*, and *piwi*-related machinery) and ovarian markers (*zp* related, *figla*, *org*, *foxl2*, and *cyp19a1a*), demonstrating that these developing gonads were in an ovarian state. In addition, genes pertaining to transforming growth factor β (TGF-β) signaling, including *bmp15*, *dvr1*, *foxh1*, *gdf2*, and *gdf9*, were also overexpressed in these individuals, some of which have been shown to be important for ovarian follicle development in zebrafish and mammals (see, e.g., Clelland and Kelly, 2011; Knight and Glister, 2006; Parrish et al., 2011). Similarly, 28 DE genes, including translational regulators (*ddx31*, *lsm14b*, *elav2*, *eif4e1b*, *pabpc1l*) and chromatin modifiers (*chtopb*, *h1m*, *setd8b*, *suv39h1a*) were identified in cluster 1. Some of these (e.g., *dazl*, *spo11*, *smc1b*, and *sycp3)* play essential roles in various aspects of meiosis (Baudat et al., 2013). In summary, our data indicated that mRNA translation and epigenetic regulation in the oocyte might be important for meiotic progression, suggesting that TGF-β signaling contributed to the development of meiotic oocytes and ovarian follicles. Several transcription factors were identified in cluster 1 as potential activators involved in profemale development. Some of them, including *sox19b* and *zglp1*, are required for ovary or granulosa cell development in various species (Li et al., 2007; Navarro-Martín et al., 2012).

Among 193 genes overexpressed in WT and PGC-depleted transforming males (clusters 4 and 5; Table S3), 20 were upregulated over 3-fold, and nine of them were uncharacterized (for a selected set, see Table S4).

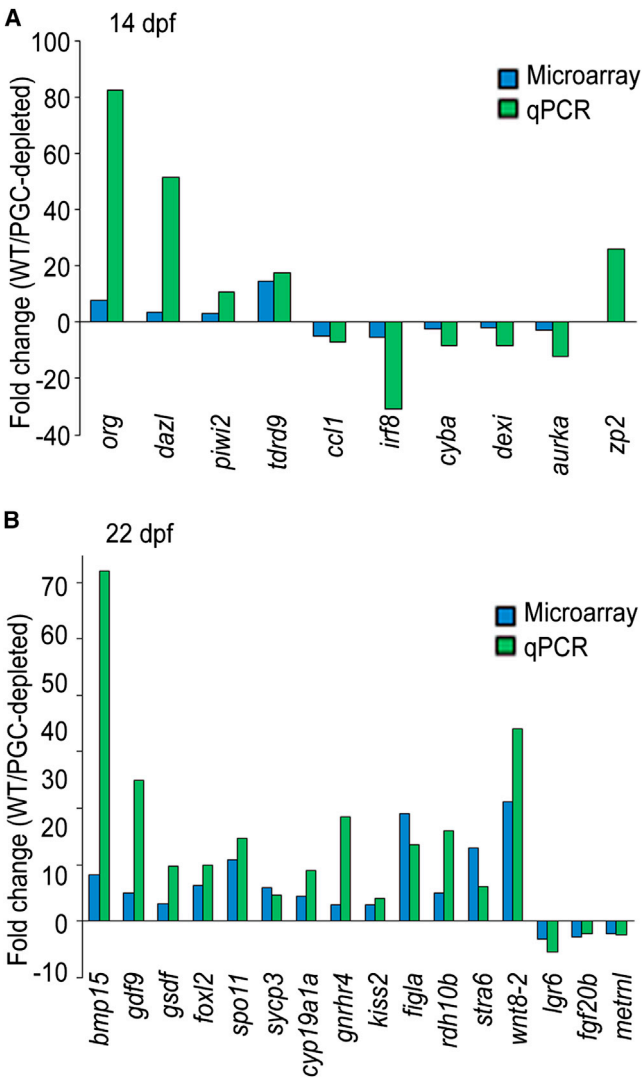

Figure 5. Validation of a Selected Set of DE Genes Identified from Microarray Data Analyses with qRT-PCR Assay

(A) 14 dpf.

(B) 22 dpf ($\geq$1.5-fold, $p < 0.05$, Student's t test).

See also Table S5 for primer sequences and Table S6 for detailed expression data.

To further investigate the transforming process of gonads, cluster 2 was compared with clusters 3 and 4. There was a total of 50 DE genes and 30 of them upregulated in cluster 2 (>2-fold, $p < 0.05$). Among the subset of 20 genes upregulated in clusters 3 and 4 were several potential testis markers, including *rnf14-like* (*loc100333926*), *rtn4b*, *cyb5r1*, and *metrnl* (Oatley et al., 2009; Zhou et al., 2002) (for a selected set, see Table S4).

To validate the microarray data, we examined the expression profiles of a selected set of DE genes and several candidate sex associated genes by a quantitative PCR (qPCR) array. A total of 26 and 107 genes was tested for 14 dpf and 22 dpf, respectively, and nearly 70% of them were verified (Figures 5A and 5B; see Table S5 for primers and Table S6 for detailed results). We identified the upregulation of *zp2* in WT samples and *star* (Leydig cell marker) in PGC-depleted gonads at 14 dpf. In contrast, we did not detect differential expression in *amh*, *sox9a* (Sertoli cell marker), and *star* at 22 dpf consistent with microarray data.

PGC-Depleted Gonads May Undergo a Less Distinct "Juvenile Ovary to Testis" Transformation

To ask whether PGC-depleted gonads differentiate in the same manner as those of WT, histological analysis was performed at different developmental stages. At 15 dpf, WT gonads contained different types of germ cells, including meiotic germ cells suggestive of the early stage of primary oocytes (Figure 6A, see inset). However, no mature, differentiated germ cells were observed in PGC-depleted gonads (Figure 6B), indicating that they were underdeveloped. This observation was consistent with confocal imaging of gonads with severely depleted PGCs, in which no clear structures were observed at 14 dpf (Figure 2B). At 23 dpf, in sharp contrast to the gonads of WT individuals (Figure 6C), there were no perinucleolar oocytes identified in PGC-depleted gonads (Figure 6D). By 28 dpf, WT gonads contained packed perinucleolar oocytes (Figure 6E). However, PGC-depleted gonads showed a range of morphologies during differentiation; some had developed ovarian structures (Figure 6F), while others solely contained germ cells with one or multiple nucleoli in the nucleus (Figure 6G). At 35 dpf, signs of apoptosis were observed, indicative of gonad transformation (Figure S3). No difference was observed between adult PGC-depleted and WT gonads (Figure S4).

Taken together, our histological findings suggest that WT gonadal primordium first develops into an immature ovary with different types of germ cells at 2 wpf. The number and size of perinucleolar oocytes may provide good indicators for ovarian maturation at later stages. In contrast, the development of PGC-depleted gonads appeared to be delayed and inadequate compared with WT. Moreover, PGC-depleted individuals may exhibit a less pronounced or shorter juvenile ovary stage during sexual differentiation. Thus, we propose that gonadal transformation may serve as a checkpoint to ensure the developmental stability of ovaries or testes.

DISCUSSION

In this report, we show that a dimorphic increase of germ cells occurs in the early larvae of zebrafish, similar to Japanese medaka (Satoh and Egami, 1972). Our data show that there is little change in the germ cell number during the

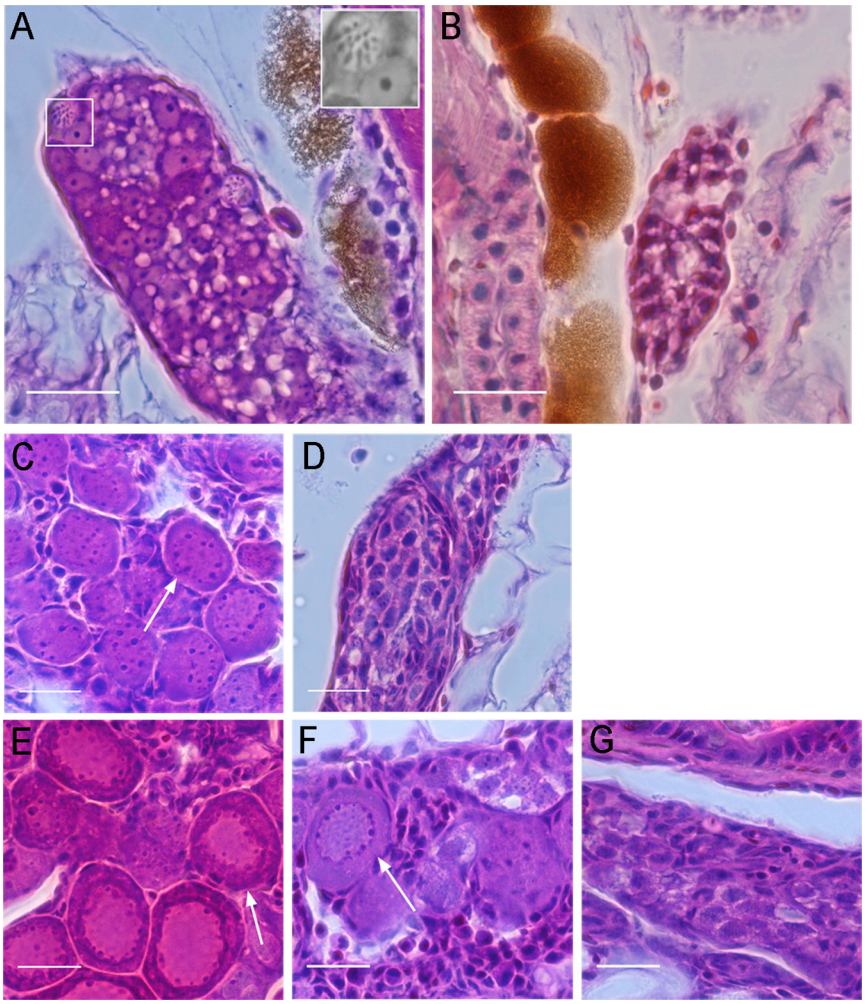

Figure 6. Hematoxylin and Eosin Staining of WT and PGC-Depleted Zebrafish Gonads at Different Developmental Stages

(A) WT gonads at 15 dpf contained meiotic germ cells indicating oogonia (white box, inset).

(B) PGC-depleted gonads at 15 dpf did not contain differentiated germ cells.

(C and D) At 23 dpf, WT (C) and PGC-depleted gonads (D) are shown. Perinucleolar oocytes were only identified in the WT gonad (arrow). PGC-depleted gonads contained germ cells with one to several nucleoli.

(E) WT gonads at 28 dpf showed slightly packed oocytes at the perinucleolar stage (arrow).

(F and G) At 28 dpf, some PGC-depleted gonads have developed ovarian structures with perinucleolar oocytes (F, arrow), whereas others were similar histologically to PGC-depleted gonads of 23 dpf (compare G and D).

Scale bars represent 20 μm. See also Figures S3 and S4.

first week of development. However, two distinct germ cell populations appear between 7 and 14 dpf, and this is strongly correlated with the resulting sex ratios of progeny. Thus, we propose that a sex-specific proliferation of germ cells marks the beginning of gonadal differentiation in zebrafish and individuals with a high PGC number have an increased propensity for the female fate.

We used two complementary methods, MO-based knockdown and cell transplantation, to generate zebrafish containing a spectrum of PGC numbers. Our findings revealed that a threshold number of PGCs is required for the stability of ovarian fate. Furthermore, no compensatory proliferation of germ cells in the PGC-depleted morphants was observed, thus maintaining the morpholino-induced phenotype during development. In organogenesis, the number of tissue-specific stem cells might regulate the final size of the organs (Stanger et al., 2007). Our results suggest that the ability of PGCs to proliferate is constrained by their number, which consequently changes the size and identity of the gonad. The development of PGC-depleted gonads appeared to be inadequate and protracted, which seems to delay differentiation further. When PGC number increased, compensatory growth occurred, indicating the presence of potential feedback molecules, possibly growth factors derived from somatic cells. Interestingly, we also observed 10%–20% of zebrafish with a PGC number below the threshold developed as females, suggesting that these individuals might possess a distinct genetic makeup, leading to different response to the size of germ cell pool. We do not know whether there is any connection between the initial PGC count and the response to the depletion. It is possible that the "additional males" appearing in the MO-depleted batch are genetic females with a lower number of initial PGCs (within the normal female range) prior to injection that forced them to develop a testis.

Germ cell sex determination and meiotic initiation are tightly coupled events during the early stage of sexual differentiation (Lesch and Page, 2012). Our histological analysis and gene expression profiles (*zp2*, *org*, *sycp3*, *dazl*) confirmed that zebrafish gonads are in a meiotic ovarian

stage at 14 dpf. Concurrently, we also detected putative testis markers expressed in WT gonads, indicating the plastic nature of early immature gonads expressing "lineage priming" genes of both sexes as shown in mammals (Jameson et al., 2012). Comparative transcriptome analysis showed that under unbiased selection, WT individuals display similar expression patterns, indicating that zebrafish undergoing either mode of proliferation (and with either sexual fate) will enter meiosis. On the other hand, PGC-depleted gonads were not able to express ovarian or meiotic markers at that stage; thus, the juvenile ovary stage might be accordingly delayed. In mammals, the mutual antagonism between CYP26B1/FGF9 and retinoic acid (RA) regulates the meiotic entry of germ cells (Kocer et al., 2009). Our data suggest that zebrafish might use alternative molecules or mechanisms for executing meiosis since we did not detect dimorphic expression of *cyp26a1* either at the beginning of sexual differentiation (14 dpf) or during meiotic progression of ovary (22 dpf). It should be noted that immune response genes were predominantly upregulated in PGC-depleted morphants at 14 dpf, and this may correlate with PGC depletion inducing a regenerative response similar to that of injured tissues (Godwin and Brockes, 2006). Moreover, we observed that immune response genes were upregulated in both WT and the PGC-depleted morphants at 22 dpf, suggesting that these genes may serve key regulatory roles during gonadal development, as in rainbow trout (Yano et al., 2012).

The comparison of transcriptomes among WT zebrafish identified seven DE genes at 14 dpf and 945 DE genes at 22 dpf, manifesting the increasing divergence of promale versus profemale pathways during development. At 22 dpf, the expression of multiple signaling pathways revealed a complex regulatory network in gonadal differentiation. Several developmental pathways have been shown to be involved in germline development and the juvenile ovary to testis transformation in zebrafish, including the canonical Wnt, Tp53/Fancl, nuclear factor-κB, and Piwi/piRNA pathways (Houwing et al., 2007; Pradhan et al., 2012; Rodríguez-Marí et al., 2010; Sreenivasan et al., 2014). Our data demonstrate that genes/pathways supporting ovarian follicle development are coupled with genes associated with meiotic progression and mRNA translation, further promoting the female fate.

Histological analysis showed the quantitative difference in perinucleolar oocytes between WT and PGC-depleted *dnd* morphants, consistent with the observation that the ratio of perinucleolar oocytes in total germ cells dictates gonadal fate (Uchida et al., 2002). Our findings suggest that oocyte meiosis is important for ovarian development. It has been reported that sex reversal in medaka occurs during meiosis (Shibata and Hamaguchi, 1988). Similarly, as shown in *fancl* mutants, only oocytes surviving through meiosis support ovarian differentiation in zebrafish (Rodríguez-Marí et al., 2010). Additionally, meiotic germ cells strengthen the ovarian fate by antagonizing the testicular pathway or triggering the maturation of somatic cells in mice (Maatouk et al., 2013; Yao et al., 2003). Thus, based on our data, a higher number of PGCs would provide more meiotic oocytes or oocyte-derived signals in sexual differentiation (Rodríguez-Marí and Postlethwait, 2011), further promoting or maintaining female fate as evidenced by the upregulation of *cyp19a1a*, *foxl2* and other profemale genes/pathways.

Gonadal Transformation May Function as a Buffering System for Developmental Outcome

It has been indicated that testicular differentiation exhibits variability in zebrafish and that all males develop "juvenile ovaries" before the initiation of testis formation (Wang et al., 2007). The earliest reported upregulation of known male sex markers, including *amh*, *sox9a*, or *cyp11c1* (earlier *cyp11b* or *cyp11b2*), and downregulation of *cyp19a1a* (a well-known female marker) in the transforming zebrafish gonads was from 30 dpf onward (Rodríguez-Marí et al., 2005; Wang and Orban, 2007). In line with these findings, we have not observed differences between the WT transforming gonads and PGC-depleted morphants at 22 dpf. On the other hand, several potential testis markers were identified. Reciprocal expression of *cyp19a1a* and *amh* during gonadal transformation might indicate transdifferentiation from granulosa cells to Sertoli cells in zebrafish (Wang and Orban, 2007). Our data suggest that germ cells in PGC-depleted gonads were not able to activate/maintain *cyp19a1a* expression in somatic cells, and *amh* expression has not yet been upregulated. Further, histological analysis showed no oocyte or ovarian structures in PGC-depleted morphants at 23 dpf, and the gonads have embarked on male differentiation via the expression of some potential testicular markers and/or the downregulation of ovary associated genes. It has been suggested that gonadal development of zebrafish without PGCs progresses with similar timing as WT (Siegfried and Nüsslein-Volhard, 2008). However, we observed different histological patterns in the PGC-depleted gonads at later stages, and PGC-depleted individuals coclustered with a subset of WT transforming males based on their 22 dpf transcriptomes, confirming the variability in testicular differentiation. Thus, we propose that gonadal transformation may function as a buffering process for stabilizing the developmental outcome of an ovary or a testis, complementing the "sexual canalization" concept championed by others (Saito and Tanaka, 2009).

A Germ Cell Number Model for Sexual Differentiation

In this study, we provide evidence that dimorphic germ cell proliferation is the first sign of sexual differentiation, and

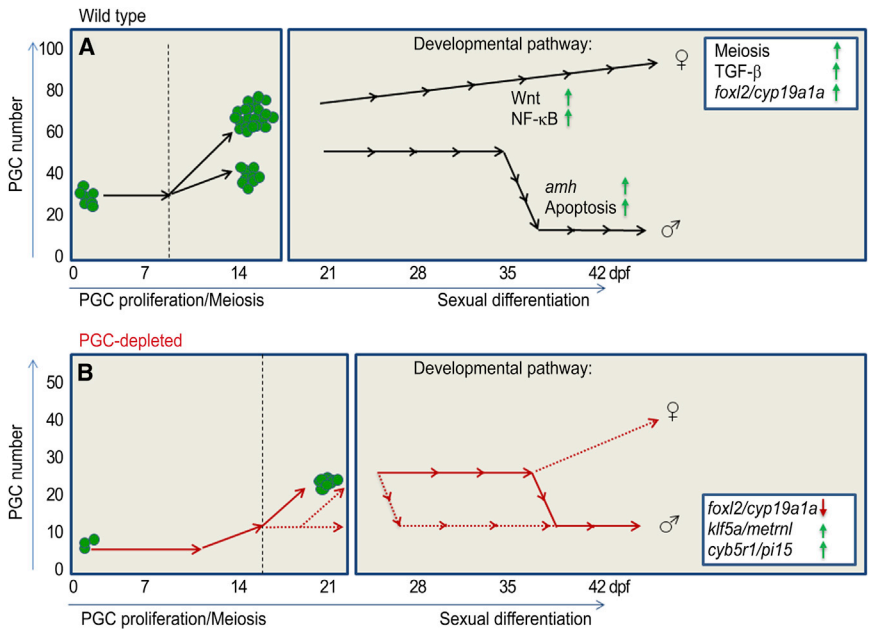

Figure 7. A Working Model for Zebrafish Sexual Differentiation: PGC Numbers Alter the Gonadal Fate

(A) This model shows that in zebrafish the beginning of gonadal differentiation occurs between 7 and 14 dpf, by which point the WT population will exhibit a bimodal distribution of individuals based on PGC number and manifest the inception of the juvenile ovary stage based on molecular markers (as identified by transcriptome). Sex ratio evaluation suggests that most individuals with low PGC number will develop as males, while those with high PGC number as females.

(B) In PGC-depleted embryos (red lines), most zebrafish develop as males, indicating that the effect caused by morpholino injection (at 24 hpf) is maintained through the development. However, 10%–20% of individuals with depleted PGC number (count 1–9) will develop as females. By 22 dpf, differences in gonadal morphology and gene expression profiles between WT and PGC-depleted transforming males can be observed. The onset and duration of this divergence vary among individuals. The "juvenile ovary" stage might be delayed or become shorter and less distinct in PGC-depleted individuals. The profemale and promale pathways reported by others are shown.

In this study, we identified potential novel factors contributing to sexual differentiation based on transcriptome and phenotype analysis (green arrows, upregulation; red arrows, downregulation, inset box). (A) was modified from Figure 1 of Orban et al. (2009) with permission.

the number of germ cells is important for stability of ovarian fate. We further demonstrate that the presence of a higher number of oocytes passing through meiosis (which may generate an increased amount of oocyte-derived signals) is important for maintenance of female development (Rodríguez-Marí and Postlethwait, 2011). On the other hand, the development of the PGC-depleted gonads appears to be slower and often incomplete, likely causing further changes in the course of testicular differentiation. Our data suggest that PGC-depleted individuals may undergo a less pronounced "juvenile ovary" stage, differing in timing and length relative to their WT counterparts (Figure 7). In conclusion, our work suggests that germ cell number plays an active role during sexual differentiation and may directly regulate the progression of gonadal transformation in zebrafish.

EXPERIMENTAL PROCEDURES

Ethics and Zebrafish Strains

The study was carried out in accordance with the Guide for the Care and Use of Laboratory Animals in Hokkaido University and Institutional Animal Care and Usage Committee at Temasek Life Sciences Laboratory. Zebrafish were kept under standard conditions and staged according to (Kimmel et al., 1995). The zebrafish strains used for the experiments were AB WT, golden mutant, *Tg(vasa:DsRed2-vasa)*; *Tg(bactin:EGFP)* double transgenic line (Wong et al., 2011), and *Tg(vasa:vasa-EGFP)*, also known as *zf45Tg* transgenic line (Krøvel and Olsen, 2002).

Generation of Germ Cell-Deficient Zebrafish

Two different methods, MO injection and cell transplantation, were used to generate PGC-deficient zebrafish. Our preliminary tests with a control MO have shown that the microinjection itself does not exert a systematic effect on gonadal development (Figure S2). Details are in the Supplemental Experimental Procedures.

Quantitation of PGC Number in Early Embryos

The suitability of determining PGC number by the squash preparation method was initially validated by comparing PGC counts obtained by this approach with those obtained by precise quantification of fluorescence intensity. Both techniques yielded numbers that were in good agreement (for details, see the Supplemental Experimental Procedures).

Confocal Microscopy

The isolated trunk region of a larva containing the prospective gonad without internal organs was embedded in 1.5% low melting agarose on a 0.17 mm coverslip and imaged on a Leica SP5 inverted confocal microscope (for details, see the Supplemental Experimental Procedures).

Quantitative Image Analysis of PGCs

To determine the number of PGCs present in each sample, confocal z stacks were analyzed using Imaris 7.4 Spot Count

function (Bitplane, Andor) using a minimum size of 5.0 μm, a positive threshold for channel 1 (excitation 488 nm) and a negative threshold for channel 2 (excitation 561 nm). The presence or absence of loose aggregates of cells or intact gonadal structures was scored visually in 3D using Imaris.

Histology

The histological analysis was performed as described (Wang et al., 2007) with modifications (for details, see the Supplemental Experimental Procedures).

Microarray-Based Transcriptome Profiling

A customized microarray was used for gene expression profiling. The microarray was designed based on various resources and manufactured by Roche NimbleGen on its 12 × 135 array format with each array containing 117,915 probes. Each probe is 60 bp and mapped to Ensembl 70 (released on January 2013). At both developmental stages, 10 samples were from PGC-depleted (1–9) morphants, and 14 samples were from randomly selected WT individuals.

Collection and Preparation of RNA Samples

All samples used for RNA extraction were from the FI family, which produces progeny sex ratio of 40% male. PGC-depleted morphants and uninjected WT were grown to the desired stages (standard length of 4–5 mm and 6–7 mm for 14 dpf and 22 dpf, respectively). The developing trunk regions without internal organs, between the opercula and anal pores, were carefully dissected. The samples were immediately snap frozen in liquid nitrogen and then stored at −80°C. For detailed information on RNA sample preparation and processing, see the Supplemental Experimental Procedures.

Microarray Data Analysis

Detailed information on microarray analysis can be found in the Supplemental Experimental Procedures.

Quantitative RT-PCR for Validation of Microarray Data

Quantitative RT-PCR was carried out using the BioMark HD system (Fluidigm). Trunk sections as opposed to isolated gonads were used, as experimental validation has proven that the presence of other tissues did not have a substantial effect on the gonadal expression level of most genes (Table S7). For detailed information on quantitative RT-PCR (qRT-PCR) assay, see the Supplemental Experimental Procedures.

ACCESSION NUMBERS

The microarray data have been deposited in the GEO database under accession number GSE57046.

SUPPLEMENTAL INFORMATION

Supplemental Information includes Supplemental Experimental Procedures, four figures, seven tables, and two movies and can be found with this article online at http://dx.doi.org/10.1016/j.stemcr.2014.10.011.

AUTHOR CONTRIBUTIONS

M.S.H., R.S., and L.O. conceived the project. K.-W.T., R.G., R.S., M.S.H., M.C., and L.O. conceived and designed experiments. K.-W.T., R.G., J.M.S., T.S., R.S., M.S.H., and M.C. performed the experiments. K.-W.T., R.G., J.M.S., R.S., M.C., K.A., E.Y., M.S.H., and L.O. analyzed and discussed the data. K.-W.T., R.G., M.C., and L.O. wrote the paper.

ACKNOWLEDGMENTS

We would like to thank Lisbeth Olsen and Paul Collodi for transgenic lines and Fiona Chia, Xianke Shi, and Daniel Koch for experimental support. Special thanks are given to Kellee Siegfried, Gerd Maack, and Helmut Segner for advice on histological sections, the members of the Orban lab for discussions, and Woei Chang Liew for constructive criticisms on the earlier versions of the manuscript. This work was supported by grants from the Temasek Life Sciences Laboratory and the Agri-Food and Veterinary Authority of Singapore (to L.O.), by PROBRAIN (Promotion of Basic Research Activities for Innovative Biosciences; to E.Y.), by a Grant-in-Aid for Young Scientists (B 18780140 to R.G.), and by the F3 Project Support Office for Female Researchers at Hokkaido University (to R.G.).

Received: April 15, 2014
Revised: October 21, 2014
Accepted: October 22, 2014
Published: November 26, 2014

REFERENCES

Baudat, F., Imai, Y., and de Massy, B. (2013). Meiotic recombination in mammals: localization and regulation. Nat. Rev. Genet. *14*, 794–806.

Clelland, E.S., and Kelly, S.P. (2011). Exogenous GDF9 but not Activin A, BMP15 or TGFβ alters tight junction protein transcript abundance in zebrafish ovarian follicles. Gen. Comp. Endocrinol. *171*, 211–217.

Dranow, D.B., Tucker, R.P., and Draper, B.W. (2013). Germ cells are required to maintain a stable sexual phenotype in adult zebrafish. Dev. Biol. *376*, 43–50.

Fujimoto, T., Nishimura, T., Goto-Kazeto, R., Kawakami, Y., Yamaha, E., and Arai, K. (2010). Sexual dimorphism of gonadal structure and gene expression in germ cell-deficient loach, a teleost fish. Proc. Natl. Acad. Sci. USA *107*, 17211–17216.

Godwin, J.W., and Brockes, J.P. (2006). Regeneration, tissue injury and the immune response. J. Anat. *209*, 423–432.

Goto, R., Saito, T., Takeda, T., Fujimoto, T., Takagi, M., Arai, K., and Yamaha, E. (2012). Germ cells are not the primary factor for sexual fate determination in goldfish. Dev. Biol. *370*, 98–109.

Houwing, S., Kamminga, L.M., Berezikov, E., Cronembold, D., Girard, A., van den Elst, H., Filippov, D.V., Blaser, H., Raz, E., Moens, C.B., et al. (2007). A role for Piwi and piRNAs in germ cell maintenance and transposon silencing in Zebrafish. Cell *129*, 69–82.

Jameson, S.A., Natarajan, A., Cool, J., DeFalco, T., Maatouk, D.M., Mork, L., Munger, S.C., and Capel, B. (2012). Temporal transcriptional profiling of somatic and germ cells reveals biased lineage

priming of sexual fate in the fetal mouse gonad. PLoS Genet. *8*, e1002575.

Kanehisa, M., Goto, S., Sato, Y., Furumichi, M., and Tanabe, M. (2012). KEGG for integration and interpretation of large-scale molecular data sets. Nucleic Acids Res. *40*, D109–D114.

Kimmel, C.B., Ballard, W.W., Kimmel, S.R., Ullmann, B., and Schilling, T.F. (1995). Stages of embryonic development of the zebrafish. Dev. Dyn. *203*, 253–310.

Knight, P.G., and Glister, C. (2006). TGF-beta superfamily members and ovarian follicle development. Reproduction *132*, 191–206.

Kocer, A., Reichmann, J., Best, D., and Adams, I.R. (2009). Germ cell sex determination in mammals. Mol. Hum. Reprod. *15*, 205–213.

Krøvel, A.V., and Olsen, L.C. (2002). Expression of a vas:EGFP transgene in primordial germ cells of the zebrafish. Mech. Dev. *116*, 141–150.

Kurokawa, H., Saito, D., Nakamura, S., Katoh-Fukui, Y., Ohta, K., Baba, T., Morohashi, K., and Tanaka, M. (2007). Germ cells are essential for sexual dimorphism in the medaka gonad. Proc. Natl. Acad. Sci. USA *104*, 16958–16963.

Lesch, B.J., and Page, D.C. (2012). Genetics of germ cell development. Nat. Rev. Genet. *13*, 781–794.

Lewis, Z.R., McClellan, M.C., Postlethwait, J.H., Cresko, W.A., and Kaplan, R.H. (2008). Female-specific increase in primordial germ cells marks sex differentiation in threespine stickleback *(Gasterosteus aculeatus*). J. Morphol. *269*, 909–921.

Li, S., Lu, M.M., Zhou, D., Hammes, S.R., and Morrisey, E.E. (2007). GLP-1: a novel zinc finger protein required in somatic cells of the gonad for germ cell development. Dev. Biol. *301*, 106–116.

Liew, W.C., and Orban, L. (2014). Zebrafish sex: a complicated affair. Brief Funct. Genomics *13*, 172–187.

Liew, W.C., Bartfai, R., Lim, Z., Sreenivasan, R., Siegfried, K.R., and Orban, L. (2012). Polygenic sex determination system in zebrafish. PLoS ONE *7*, e34397.

Maatouk, D.M., Mork, L., Chassot, A.A., Chaboissier, M.C., and Capel, B. (2013). Disruption of mitotic arrest precedes precocious differentiation and transdifferentiation of pregranulosa cells in the perinatal Wnt4 mutant ovary. Dev. Biol. *383*, 295–306.

Matson, C.K., Murphy, M.W., Sarver, A.L., Griswold, M.D., Bardwell, V.J., and Zarkower, D. (2011). DMRT1 prevents female reprogramming in the postnatal mammalian testis. Nature *476*, 101–104.

Merchant-Larios, H., and Centeno, B. (1981). Morphogenesis of the ovary from the sterile W/Wv mouse. Prog. Clin. Biol. Res. *59B*, 383–392.

Mi, H., Muruganujan, A., Casagrande, J.T., and Thomas, P.D. (2013). Large-scale gene function analysis with the PANTHER classification system. Nat. Protoc. *8*, 1551–1566.

Navarro-Martín, L., Galay-Burgos, M., Piferrer, F., and Sweeney, G. (2012). Characterisation and expression during sex differentiation of Sox19 from the sea bass *Dicentrarchus labrax*. Comp. Biochem. Physiol. B Biochem. Mol. Biol. *163*, 316–323.

Oatley, J.M., Oatley, M.J., Avarbock, M.R., Tobias, J.W., and Brinster, R.L. (2009). Colony stimulating factor 1 is an extrinsic stimulator of mouse spermatogonial stem cell self-renewal. Development *136*, 1191–1199.

Orban, L., Sreenivasan, R., and Olsson, P.E. (2009). Long and winding roads: testis differentiation in zebrafish. Mol. Cell. Endocrinol. *312*, 35–41.

Parrish, E.M., Siletz, A., Xu, M., Woodruff, T.K., and Shea, L.D. (2011). Gene expression in mouse ovarian follicle development in vivo versus an ex vivo alginate culture system. Reproduction *142*, 309–318.

Pradhan, A., Khalaf, H., Ochsner, S.A., Sreenivasan, R., Koskinen, J., Karlsson, M., Karlsson, J., McKenna, N.J., Orbán, L., and Olsson, P.E. (2012). Activation of NF-κB protein prevents the transition from juvenile ovary to testis and promotes ovarian development in zebrafish. J. Biol. Chem. *287*, 37926–37938.

Rodríguez-Marí, A., and Postlethwait, J.H. (2011). The role of Fanconi anemia/BRCA genes in zebrafish sex determination. Methods Cell Biol. *105*, 461–490.

Rodríguez-Marí, A., Yan, Y.L., Bremiller, R.A., Wilson, C., Cañestro, C., and Postlethwait, J.H. (2005). Characterization and expression pattern of zebrafish Anti-Müllerian hormone (Amh) relative to *sox9a, sox9b,* and *cyp19a1a*, during gonad development. Gene Expr. Patterns *5*, 655–667.

Rodríguez-Marí, A., Cañestro, C., Bremiller, R.A., Nguyen-Johnson, A., Asakawa, K., Kawakami, K., and Postlethwait, J.H. (2010). Sex reversal in zebrafish fancl mutants is caused by Tp53-mediated germ cell apoptosis. PLoS Genet. *6*, e1001034.

Saito, D., and Tanaka, M. (2009). Comparative aspects of gonadal sex differentiation in medaka: a conserved role of developing oocytes in sexual canalization. Sex Dev. *3*, 99–107.

Saito, D., Morinaga, C., Aoki, Y., Nakamura, S., Mitani, H., Furutani-Seiki, M., Kondoh, H., and Tanaka, M. (2007). Proliferation of germ cells during gonadal sex differentiation in medaka: Insights from germ cell-depleted mutant zenzai. Dev. Biol. *310*, 280–290.

Saito, T., Goto-Kazeto, R., Arai, K., and Yamaha, E. (2008). Xenogenesis in teleost fish through generation of germ-line chimeras by single primordial germ cell transplantation. Biol. Reprod. *78*, 159–166.

Satoh, N., and Egami, N. (1972). Sex differentiation of germ cells in the teleost, Oryzias latipes, during noraml embryonic development. J. Embryol. Exp. Morphol. *28*, 385–395.

Shibata, N., and Hamaguchi, S. (1988). Evidence for the sexual bipotentiality of spermatogonia in the fish, *Oryzias latipes*. J. Exp. Zool. *245*, 71–77.

Siegfried, K.R., and Nüsslein-Volhard, C. (2008). Germ line control of female sex determination in zebrafish. Dev. Biol. *324*, 277–287.

Slanchev, K., Stebler, J., de la Cueva-Méndez, G., and Raz, E. (2005). Development without germ cells: the role of the germ line in zebrafish sex differentiation. Proc. Natl. Acad. Sci. USA *102*, 4074–4079.

Sreenivasan, R., Jiang, J., Wang, X., Bártfai, R., Kwan, H.Y., Christoffels, A., and Orbán, L. (2014). Gonad differentiation in zebrafish is regulated by the canonical Wnt signaling pathway. Biol. Reprod. *90*, 45.

Stanger, B.Z., Tanaka, A.J., and Melton, D.A. (2007). Organ size is limited by the number of embryonic progenitor cells in the pancreas but not the liver. Nature *445*, 886–891.

Takahashi, H. (1974). Juvenile hermaphroditism in the zebrafish, *Brachydanio rerio*. Bull. Fac. Fish. Hokkaido Univ. *28*, 57–65.

Uchida, D., Yamashita, M., Kitano, T., and Iguchi, T. (2002). Oocyte apoptosis during the transition from ovary-like tissue to testes during sex differentiation of juvenile zebrafish. J. Exp. Biol. *205*, 711–718.

Uhlenhaut, N.H., Jakob, S., Anlag, K., Eisenberger, T., Sekido, R., Kress, J., Treier, A.C., Klugmann, C., Klasen, C., Holter, N.I., et al. (2009). Somatic sex reprogramming of adult ovaries to testes by FOXL2 ablation. Cell *139*, 1130–1142.

Wang, X.G., and Orban, L. (2007). Anti-Müllerian hormone and 11 beta-hydroxylase show reciprocal expression to that of aromatase in the transforming gonad of zebrafish males. Dev. Dyn. *236*, 1329–1338.

Wang, X.G., Bartfai, R., Sleptsova-Freidrich, I., and Orban, L. (2007). The timing and extent of "juvenile ovary" phase are highly varible during zebrafish testis differentiation. J. Fish Biol. *70*, 33–44.

Warr, N., and Greenfield, A. (2012). The molecular and cellular basis of gonadal sex reversal in mice and humans. Wiley Interdiscip. Rev. Dev. Biol. *1*, 559–577.

Wilson, C.A., High, S.K., McCluskey, B.M., Amores, A., Yan, Y.L., Titus, T.A., Anderson, J.L., Batzel, P., Carvan, M.J., III, Schartl, M., et al. (2014). Wild sex in zebrafish: loss of the natural sex determinant in domesticated strains. Genetics. Published online September 18, 2014. http://dx.doi.org/10.1534/genetics114169284.

Wong, T.T., Saito, T., Crodian, J., and Collodi, P. (2011). Zebrafish germline chimeras produced by transplantation of ovarian germ cells into sterile host larvae. Biol. Reprod. *84*, 1190–1197.

Yano, A., Guyomard, R., Nicol, B., Jouanno, E., Quillet, E., Klopp, C., Cabau, C., Bouchez, O., Fostier, A., and Guiguen, Y. (2012). An immune-related gene evolved into the master sex-determining gene in rainbow trout, *Oncorhynchus mykiss*. Curr. Biol. *22*, 1423–1428.

Yao, H.H., DiNapoli, L., and Capel, B. (2003). Meiotic germ cells antagonize mesonephric cell migration and testis cord formation in mouse gonads. Development *130*, 5895–5902.

Zhou, Z.M., Sha, J.H., Li, J.M., Lin, M., Zhu, H., Zhou, Y.D., Wang, L.R., Zhu, H., Wang, Y.Q., and Zhou, K.Y. (2002). Expression of a novel reticulon-like gene in human testis. Reproduction *123*, 227–234.

Stem Cell Reports, Volume *4*

Supplemental Information

Early Depletion of Primordial Germ Cells in Zebrafish Promotes Testis Formation

Keh-Weei Tzung, Rie Goto, Jolly M. Saju, Rajini Sreenivasan, Taiju Saito, Katsutoshi Arai, Etsuro Yamaha, Mohammad Sorowar Hossain, Meredith E.K. Calvert, and László Orbán

Supplemental Figures

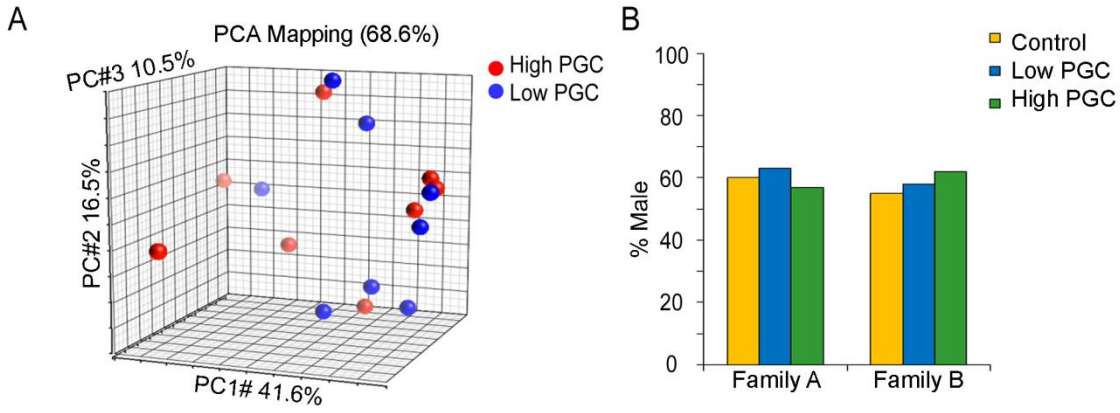

Figure S1: PGC counts at 28-32 hpf in uninjected individuals are not predictive of sexual development, as determined by later trunk-based gene expression profiles and adult sex ratios. Related to Figure 2. (A) Uninjected individuals from the *Tg(vasa:vasa-EGFP)* line were sorted to low and high PGC counts at 28–32 hpf. Eight trunk samples each from the above groups were collected at 22 dpf and analyzed by a qRT-PCR assay using a panel containing 90 pairs of primers designed for 70 genes. A fully overlapping set of points from the 'early high' and 'early low' PGC samples on the PCA plot can be observed. (B) Individuals from two *Tg(vasa:vasa-EGFP)* families (Family A & B) were sorted to high and low PGC group at 28–32 hpf and were grown to 46 dpf to evaluate their sex ratio. The sex ratio of both sorted groups were similar to those of unsorted controls in both families (Family A, n = 163, 78, 72 and Family B, n = 158, 58, 62 for control, low PGC and high PGC, respectively).

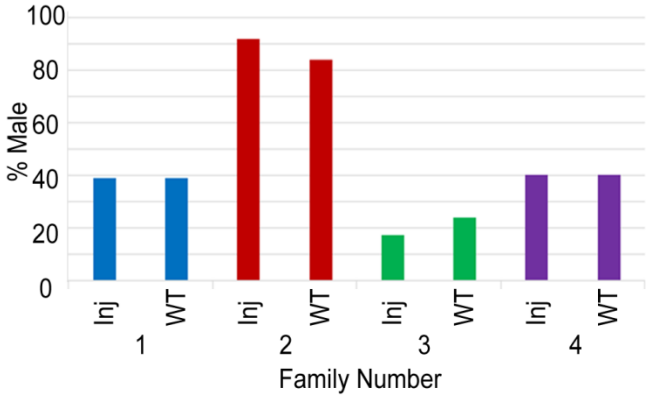

Figure S2: Microinjection with a control morpholino at zygotic stage does not change the adult sex ratio of zebrafish. Related to Figure 2. Zygotes from four different pairs of zebrafish (families #1-4) from the *Tg(vasa:vasa-EGFP)* line were injected with control MO (80 pg) targeted to the human beta-globin intron. The injected (Inj; without prior screening of PGC numbers; n = 240, 36, 35, 126) and uninjected (WT; n = 194, 183, 139, 139) individuals were grown to adulthood for sexual phenotype evaluation. The results showed that the difference between the sex ratios of the injected and the uninjected WT siblings was not statistically significant, suggesting that any effect caused by injection was minimal and random.

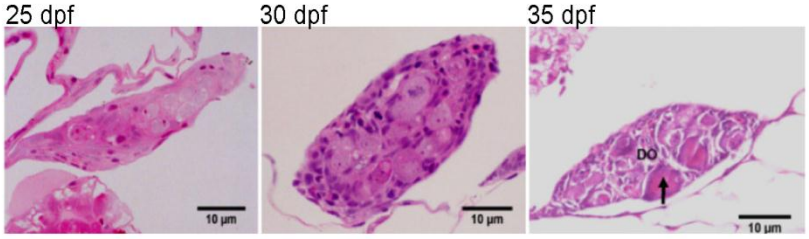

Figure S3: The gonads with heavily depleted PGC number undergo the "juvenile ovary to testis" transformation process. Related to Figure 6. To

investigate whether the development of zebrafish gonads with heavily depleted PGCs was different from that of the wild type, we performed histological analysis between 25 - 35 dpf. The results showed that the juvenile ovary stage occurred in the low PGC number (1-7) zebrafish as was observed in the uninjected control. The gonads with severely depleted PGCs had fewer oocytes but more stromal cells at 25 dpf, and the presence of degenerative oocytes (DO) was detected at 35 dpf. Scale bar: 10 µm.

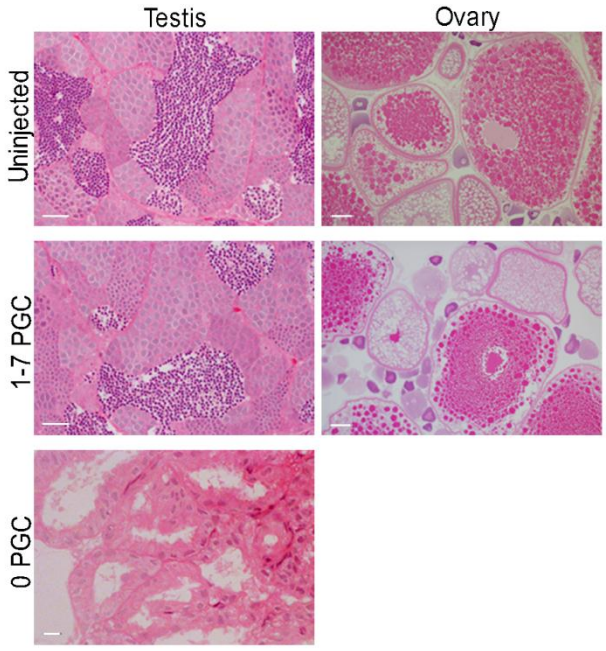

Figure S4: Adult gonads derived from zebrafish with severely depleted PGC number develop similarly to those of the uninjected control. Related to Figure 6. Histological analysis of adult gonads of manipulated zebrafish showed that the structure of both adult testes and ovaries that developed from group I embryos (1-7 PGCs) were similar to those of gonads from group IV (uninjected individuals). Primary and secondary spermatocytes and round spermatids were observed in the testis, while the ovary contained all stages of oocytes. Both adult males and females from group I were sexually active and fertile. In contrast,

zebrafish devoid of PGCs developed testicular structure without having germ cells. Scale bar: 20 μm (testis); 100 μm (ovary).

Supplemental Tables

Table S1: The survival rate of germline chimeras generated by BdT or SPT at different developmental stages. Related to Figure 3.

Method	Experimental group	No. of embryos	No. of normal embryos (%)	PGCs at genital ridge (%)	No. of fish for sexing (%)
SPT	Chimeras	141	87 (61.7)	18 (20.7)	12 (66.7)
	MO	101	89 (88.1)	N/A	60
	Control	85	81 (95.3)	N/A	63
BdT	Chimeras	527	393 (74.6)	372 (94.7*)	97 (26.1)
	MO	197	173 (87.8)	N/A	99
	Control	116	96 (82.8)	N/A	73
Total	Chimeras	608	480 (79.0)	390 (81.3)	109 (28.0)
	MO	298	260 (87.3)	N/A	159
	Control	201	177 (88.1)	N/A	136

* In BdT chimeras, the donor PGCs were present at the gonadal region in most (94.7%) of the host embryos. The rest were lost during migration and ended up at other locations (e.g., the head or the tail region). In contrast to the high success rate of the early germline chimeras, only 26.1% of BdT chimeras grew up to adulthood for the evaluation of sexual phenotypes.

Table S4 : Functional classification of a selected set of genes differentially expressed between WT and PGC-depleted morphants at 14 and 22 dpf. Related to Figure 4.

Developmental stage	Function	Gene symbols*
14dpf		
	Immune	*ccl1, cd209, cyba, irf8, loc799208, zgc:153219*
	Meiosis	*dazl, hormad1, insb, smc1, sycp2*
	Stem/Germ cells	*piwi1, piwi2, tdrd1, tdrd5, tdrd6, tdrd9*
	Cell cycle	*aurka, ccna2, cdc7, chtf18, mcm7, nuasp1*
	Translation	*eif4e1b, mex3b*
	Ovary marker	*org*
	Testis marker	*loc100149647, rnf17*
	Transcription	*snapc1a, tbpl2*
22dpf**		
	Cell death	*baxa, birc5b, bokb, card14, pdcd2, sept4a, siva1, tigara*
	Cell cycle	*btg4, ccna1, ccnb2, ccnd3, ccnh, cdc25, cdca9, fbxo43, mos, sfr1, spdya, wee2*
	Germ/Stem cells	*buc, dnd, gtsf1, henmt1,lhx8a, lin28a, nanog, nanos3,nfr,piwi1, piwi2, pou5f1, rnf17, tdrd1, tdrd12, tdrd5, tdrd6, tdrd7, tdrd9, vasa*
	Meiosis	*dazl, dmc1, hormad1, m1ap1, mei4, meiob, rad21l1, smc1b, spo11, sycp1, sycp2, sycp3, zte38*
	Insulin	*igf3, insb, lmx1a, rfx6*
	TGF-β	*bmp15, dab2, dvr1, foxh1, gdf2, gdf9, gsdf, smad3a, tgfbrap1*
	Retinoic acid	*rbp1b, rdh10b, retsatl, stra6*
	Wnt	*cby1, lgr6, pias4b, wnt8-2*
	Translation/ RNA binding	*caprin2, ddx31, ddx41, eif4e1b, elav2, lsm14b, lsm6, pabpc1l, rbm46*
	Ovary/Testis marker	*figla, foxl2, loc567678, odf3b, org,stk31, zar1, zp2, zp2.2, zp2.5, zp2l1,zp2l2,zp3, zpcx*
	Transcription factor	*ccdc106, dlx6a, drap1, foxa, klf5a, otx1b, pbx2, ripply2, six4a, sox19b, sox8, wu:fi69e09, zglp1*
	Hormone	*cyp17a2, cyp19a1a, fshr, gnrhr2, gnrhr3, gnrhr4, gphb5, hsd3b1, kiss2, pth2r, tshb*
	Immune	*ccl1, cd36, crfb12, il7r, irg1l, irgf1, isg15, ptges, tlr18, tlr3*
	Chromatin	*chtopb, h1m, habp4, npm2, setd8b, suv39h1a*
	Notch	*adam10a, dlk2, jaglb*
	Growth factor	*fgf14, fgf18a, fgf20b*
	Putative male marker	*adam19b, co355608, cyb5r1, klf5a, lin7a, loc100329403, metrnl, pi15, rtn4b, si:dkeyp-66d1.7*

* Genes in black were over-expressed in WT samples, and those in red were up-regulated in the PGC-depleted group at 14 dpf.

******For 22 dpf**,** the gene list was mainly compiled from comparisons between "immature females" vs. a subset of WT and PGC-depleted transforming males (cluster 1 vs. clusters 4&5), "immature females" vs. PGC-depleted transforming males (cluster 1 vs. cluster 5), and among transforming WT individuals (cluster 2 vs. clusters 3&4). Genes in black were up-regulated in the pro-female group, while genes in red were over-expressed in the PGC-depleted or in the pro-male group.

Table S7: Comparative expression analysis of gonad-containing and gonad-less trunks shows that most genes showing differential expression are gonad-enhanced. Related to Figure 4.

	Relative expression			**Relative expression**		
	14 dpf		**Residual**	**22 dpf**		**Residual**
Genes	**(+)gonad**	**(-)gonad**	**expression(%)**	**(+)gonad**	**(-)gonad**	**expression(%)**
birc5b	1.98	0.02	1.09	1.97	0.03	1.64
bokb	1.84	0.16	8.62	1.69	0.31	18.12
btg4	1.88	0.12	6.55	1.97	0.03	1.49
ccdc106	1.83	0.17	9.04	1.83	0.17	9.49
cyp11a1	1.94	0.06	3.33	1.69	0.31	18.28
cyp17a2#	1.98	0.02	0.94	1.55	0.45	29.18
cyp19a1a	N/A	N/A	N/A	1.57	0.24	15.30
dab	1.97	0.03	1.62	N/A	N/A	N/A
dazl	1.99	0.01	0.51	1.92	0.08	4.38
dnd	1.98	0.02	0.89	1.90	0.10	5.26
dram	1.83	0.17	9.43	1.65	0.35	21.57
dvr1	1.72	0.28	16.47	1.81	0.19	10.43
elavl2	1.75	0.00	0.22	1.66	0.09	5.40
*fgf14**	1.59	0.41	26.01	N/A	N/A	N/A
fgf18a	1.75	0.25	14.06	1.61	0.39	23.86
fgf20b	1.78	0.22	12.56	N/A	N/A	N/A
figla	N/A	N/A	N/A	1.75	0.00	0.16
foxh1	1.75	0.25	14.61	1.64	0.36	22.16
foxl2	1.93	0.07	3.58	1.69	0.31	18.65
fshr	1.95	0.05	2.32	1.49	0.26	17.33
gdf2	1.75	0.25	14.13	1.71	0.29	16.66
gdf9	1.96	0.04	2.19	1.92	0.08	4.34
gnrhr2	1.85	0.15	8.06	1.70	0.30	17.84
gnrhr3#	1.78	0.22	12.35	1.53	0.47	31.04
gsdf	1.64	0.36	21.61	1.97	0.03	1.55
gsdf2	1.94	0.06	2.83	N/A	N/A	N/A
hormad1	1.99	0.01	0.46	1.90	0.10	5.04
ihx8a	1.90	0.10	5.32	1.90	0.10	5.02
il7r#	1.79	0.21	11.5	1.55	0.45	29.21
insb	1.91	0.09	4.71	1.85	0.15	8.25
*irf8**	1.49	0.51	34.20	N/A	N/A	N/A
kiss2	1.84	0.16	8.50	N/A	N/A	N/A
*klf3**	1.49	0.51	34.67	N/A	N/A	N/A

lin28a	1.86	0.14	7.81	1.85	0.15	7.84
metrnl	1.74	0.26	14.81	1.61	0.39	24.02
mos	1.85	0.15	8.38	1.83	0.17	9.18
nanog	1.64	0.04	2.56	2.50	0.00	0.05
nanos3	1.74	0.26	15.26	1.84	0.16	8.46
nfr	1.69	0.31	18.16	1.74	0.26	15.21
npm	1.74	0.26	14.83	1.82	0.18	9.77
odf3b	1.93	0.07	3.54	1.83	0.17	9.11
org	1.93	0.07	3.64	1.96	0.04	1.92
pdcd2	1.74	0.26	15.14	1.60	0.40	24.98
pias4b	1.93	0.07	3.68	1.88	0.12	6.17
piwi1	N/A	N/A	N/A	1.88	0.12	6.15
piwi2	1.95	0.05	2.60	1.84	0.16	8.56
pou5f1	1.91	0.09	4.56	1.93	0.07	3.57
rbp1b	1.95	0.05	2.42	1.93	0.07	3.63
rdh10b#*	1.51	0.49	32.80	1.51	0.49	32.28
retsatl	2.00	0.00	0.23	1.74	0.01	0.34
rnf17	1.93	0.07	3.76	1.80	0.20	11.31
sept4a	1.71	0.29	16.68	1.82	0.18	9.67
smc1b	1.81	0.19	10.59	1.41	0.09	6.75
sox19b	1.84	0.16	8.89	1.62	0.38	23.67
sox9a	1.83	0.17	9.38	N/A	N/A	N/A
spo11	1.97	0.03	1.50	1.90	0.10	5.10
star#	1.95	0.05	2.34	1.51	0.49	32.66
stra6	1.90	0.10	5.39	1.88	0.12	6.31
sycp3l	1.95	0.05	2.33	1.88	0.12	6.20
tdrd9	1.81	0.19	10.25	1.78	0.22	12.27
wnt4a	1.83	0.17	9.11	1.76	0.24	13.71
wnt8	1.25	0.04	3.12	1.98	0.02	0.94
zp2	2.02	0.23	11.52	1.99	0.01	0.29
Muscle associated genes (positive controls)						
acta1	1.22	1.04	84.63	1.02	0.97	94.94
mylpfa	1.27	0.93	73.39	1.18	0.87	73.74
myostatin	1.22	1.04	85.77	0.93	1.05	113.66
pax3	1.07	0.93	86.18	1.22	0.78	63.85
pax7	0.93	1.07	116.13	1.10	0.86	78.53

* - > 25% residual expression in trunk (without gonad) samples collected at 14 dpf.

- > 25% residual expression in trunk (without gonad) samples collected at 22 dpf.

Supplemental Experimental Procedures

Manipulation of PGC number in zebrafish embryos

We used individuals from the *Tg*(*vasa:vasa-EGFP*) transgenic zebrafish line for investigating the role of PGCs during gonadal development. We manipulated the PGC number in zebrafish embryos by using *dead end* (*dnd*) morpholino (*dnd*-MO), as described previously (Weidinger et al., 2003). In order to achieve partially depleted PGC numbers, we first titrated concentrations of *dnd*-MO, which were microinjected into embryos at one cell stage using a PLI-100 Pico-Injector (Harvard Apparatus). The optimal concentration of *dnd*-MO required to generate embryos with various numbers of PGCs was determined to be 80-100 pg per embryo. In the *Tg(vasa:vasa-EGFP)* transgenic line, EGFP is maternally deposited in the embryos and the product of zygotic expression localizes only into the germ cells. We counted the PGC number via monitoring the GFP signal under a dissecting microscope (Leica) equipped with a fluorescent attachment (MAA-03/B; BLS Ltd, Budapest, Hungary) over the time period of 52-86 hpf. To facilitate the PGC counting, embryos were depigmented by treating them with 1-Phenyl 2-thiourea (PTU) at 24hpf.

Mass cross approach

Altogether, around 6,000 embryos from six different batches of eggs produced by mass crosses were injected with 100 pg *dnd*-MO per embryo, which yielded embryos with various numbers of PGCs. The *dnd* morphants were broadly categorized into four different groups: group I (1-7 PGCs), group II (8-15 PGCs), group III (>15 PGCs), group IV (uninjected control) and embryos with no PGC were designated as group V, which was used as control. The *dnd* morphants and uninjected embryos (control) were grown to 3 months post-fertilization (mpf) for evaluation of their sexual phenotype by (i) the differential expression of EGFP in the gonads, whereby the presence of a high level of EGFP signal was shown

earlier to correlate with ovarian differentiation, (ii) external phenotype, and (iii) occasional dissection for verification.

Pairwise cross approach

In addition, we performed pairwise crosses with a similar experimental setup as described above. Briefly, ca. 1000 embryos of the *Tg(vasa:vasa-EGFP)* zebrafish line of mating pairs with known offspring sex ratios were microinjected with *dnd*-MO (total 4 replicated experiments). The ideal concentration of *dnd* MO for generating a wide range of PGC number was 80 pg per embryo after titration. Injected embryos (without PTU treatment) were grouped based on the number of PGCs identified between 24-32 hpf under the compound epifluorescence microscope. Several groups of zebrafish including no PGC (0), low PGC number (1-6, 7-10), medium PGC number (11-20), and high PGC number (> 20) were generated. The sex ratio of *dnd* morphants was evaluated at adulthood (3 mpf).

Production of germline chimeras

To produce germline chimeras, a single PGC transplantation (SPT) and blastoderm transplantation (BdT) were performed. In general, the SPT method yields germline chimeras that possess a single donor-derived PGC with no somatic cell contamination, while BdT method was more useful to produce germline chimeras that possess more than one PGC. Detailed procedures for SPT and BdT were described elsewhere (Saito et al., 2010; Yamaha et al., 2001). Briefly, a GFP-labeled PGC was derived from a 10-15 somite embryo injected with GFP-*nos3* 3'UTR mRNA, and was subsequently transplanted into the host blastula. The resultant chimera possessed a single donor derived PGC and named as SPT chimera. For BdT chimeras, the *Tg*(*vasa:DsRed2-vasa*);*Tg*(*bactin:EGFP*) double transgenic zebrafish line was used as the donor. Therefore, the host and donor cells were easily distinguished under fluorescent microscope since donor cells started expressing GFP around the early blastula stage under driven by β-actin promoter. During the early to mid-blastula stage,

the upper half of the blastoderm was cut and removed from the host embryo. Then, the whole donor blastoderm was cut and transplanted onto the host blastula. Consequently, the donor blastoderm adhered to the recipient and became involved in its development in a few hours (Figure 3C). Both the procedure of creating BdT chimeras and the process of mixing up donor and host blastoderm were shown in Movie S1 and Movie S2.

To distinguish offspring by body color, wild type zebrafish were used as the donor and golden zebrafish as the host. All host embryos were received *dnd* -MO to deplete endogenous PGCs completely (Ciruna et al., 2002; Weidinger et al., 2003). Confirmation of complete depletion was checked by microscopic observation of empty gonads in the *dnd* morphants. The number of PGCs in each chimera was counted under the fluorescent inverted microscope (Leica DMI6000B) at the prim-5 stage. The gonads of BdT chimeras were examined to determine whether the germline chimeras only possessed RFP (+) germ cells. Each chimera was kept separately until identification of the two sexes based on phenotypic signs and/or dissection of their gonads became possible. Images of the embryos were obtained using a Leica MZ16F fluorescence stereomicroscope equipped with a digital camera (Leica DFC300FX). The gonadal phenotype of individuals developing from the germline chimeras was determined at adult by analyzing their secondary sex characteristics.

Confocal microscopy

The larval trunks embedded in 1.5% low melting agarose were imaged on a Leica SP5 inverted confocal microscope equipped with a HCX PL APO 40x/1.25 N.A. oil objective lens. Samples were illuminated with 488 nm to excite the GFP-tagged protein and with 561 nm to excite the autofluorescence of pigmented tissues, in order to remove false positives from the analysis. Due to large variations in GFP intensities and sample depth, laser power was adjusted to optimize contrast for individual samples. Confocal Z-stacks were imaged every

0.8 µm from 40-120 µm, depending on the sample thickness and the position of PGCs within the tissue.

RNA sample preparation and processing

RNA samples were extracted using Ambion RNAqueous-Micro Kit (Life Technologies). RNA quality was assessed by the Agilent 2100 Bioanalyzer with the RNA 6000 Pico LabChip (Agilent Technologies). Only samples with RIN value > 8 were used for subsequent microarray analysis. RNA concentration was quantified using Qubit 1.0 Fluorometer with RNA Assay Kit (Life Technologies).
Due to small amounts of RNA isolated from individual sample, whole transcriptome amplification (WTA) was performed prior to microarray hybridization. A total of 15 ng RNA was used for amplification with Ovation RNA Amplification System V2 (NuGEN). The size distribution of the amplified double stranded cDNA samples were checked by Agilent 2100 Bioanalyzer with RNA 6000 Nano Labchip (Agilent Technologies) to ensure fragment size uniformity among the samples.

One µg of the double stranded cDNA from each sample was labeled using NimbleGen One-Color DNA Labeling Kit (Roche NimbleGen), and hybridization was carried out according to the manufacturer's instructions. After overnight hybridization (16-20 hours), the microarray chip was washed with NimbleGen Wash Buffer Kit (Roche NimbleGen). The array was then scanned at 5 µm resolution with Axon GenePix 4000B Microarray scanner (Molecular Devices).

Microarray data analysis

The microarray data was collected and analyzed according to the MIAME standards (Brazma et al., 2001). The raw fluorescent intensity data were retrieved from the scanned images by NimbleScan version 2.6 (Roche NimbleGen) according to the manual. Robust multi-array average (Irizarry et al., 2003), quantile normalization (Bolstad et al., 2003) and background correction were applied as implemented in NimbleScan to generate the Pair files. The Pair

files were then imported into the Partek Genomics Suite version 6.6 (Partek Incorporated) for further analysis. The DE transcripts between the PGC-depleted (1-9) group and WT group were identified as significant at least 2-fold, at p <0.05 (false discovery rate-adjusted).

Quantitative RT-PCR

Specific target amplification was carried out on the cDNA (from total RNA after WTA) using TaqMan PreAmp Master Mix (Applied Biosystems), and the products were loaded onto the Fluidigm's Dynamic Array Integrated Fluidic Circuits (IFC) according to Fluidigm's EvaGreen DNA Binding Dye protocols. Six PGC-depleted morphants and ten WT samples were selected for analysis; triplicates were for each sample.

Histology

The tissues were fixed in 4% paraformaldehyde at 4˚C overnight. After dehydration, samples were embedded in HistoResin (Leica). Serial sections of 5 um were cut by microtome (Leica), dried on slides at 42˚C overnight, stained with hematoxylin and eosin (H&E), mounted in Permount (Fisher), and imaged with phase contrast with a 100x/1.4 N.A. oil objective lens.

Supplemental References

Bolstad, B.M., Irizarry, R.A., Astrand, M., and Speed, T.P. (2003). A comparison of normalization methods for high density oligonucleotide array data based on variance and bias. Bioinformatics *19*, 185-193.

Brazma, A., Hingamp, P., Quackenbush, J., Sherlock, G., Spellman, P., Stoeckert, C., Aach, J., Ansorge, W., Ball, C.A., Causton, H.C.*, et al.* (2001). Minimum information about a microarray experiment (MIAME)-toward standards for microarray data. Nat Genet *29*, 365-371.

Ciruna, B., Weidinger, G., Knaut, H., Thisse, B., Thisse, C., Raz, E., and Schier, A.F. (2002). Production of maternal-zygotic mutant zebrafish by germ-line replacement. Proc Natl Acad Sci U S A *99*, 14919-14924.

Irizarry, R.A., Hobbs, B., Collin, F., Beazer-Barclay, Y.D., Antonellis, K.J., Scherf, U., and Speed, T.P. (2003). Exploration, normalization, and summaries of high density oligonucleotide array probe level data. Biostatistics *4*, 249-264.

Saito, T., Goto-Kazeto, R., Fujimoto, T., Kawakami, Y., Arai, K., and Yamaha, E. (2010). Inter-species transplantation and migration of primordial germ cells in cyprinid fish. Int J Dev Biol *54*, 1481-1486.

Weidinger, G., Stebler, J., Slanchev, K., Dumstrei, K., Wise, C., Lovell-Badge, R., Thisse, C., Thisse, B., and Raz, E. (2003). dead end, a novel vertebrate germ plasm component, is required for zebrafish primordial germ cell migration and survival. Curr Biol *13*, 1429-1434.

Yamaha, E., Kazama-Wakabayashi, M., Otani, S., Fujimoto, T., and Arai, K. (2001). Germ-line chimera by lower-part blastoderm transplantation between diploid goldfish and triploid crucian carp. Genetica *111*, 227-236.